J Mater Sci (2008) 43:3923–3930
DOI 10.1007/s10853-007-2372-5

INTERGRANULAR AND INTERPHASE BOUNDARIES IN MATERIALS

Wear-induced microstructure in Ni/Cu nano-multilayers

Tomoya Hattori · Yoshihisa Kaneko ·
Satoshi Hashimoto

Received: 7 July 2007 / Accepted: 3 December 2007 / Published online: 21 March 2008

Abstract Sliding wear tests were carried out in order to investigate wear resistance and resultant microstructure of Ni/Cu multilayers. The Ni/Cu multilayers having the component layer thickness h ranging from 5 to 100 nm were fabricated on copper substrates using the elecrodeposition technique. It was found that the wear depths in the multilayers were less than one-fifth of that of a conventional nickel coating at a high load condition. The wear resistance of the multilayer was almost independent of the component layer thickness, except the multilayer of $h = 100$ nm whose resistance was lower than those of the others. The observation of cross section revealed that the grains were generated locally near the worn surface in the Ni/Cu multilayers. Surface cracks were grown in such grained areas. The multilayer having a large grained area showed relatively low wear resistance. From the TEM observation, there were many equiaxed grains without the laminated structure. It is conceivable that the equiaxed grains without the laminated structure were formed due to dynamic recrystallization occurring after the laminated structure was annihilated by severe deformation. Assuming that the annihilation period is required for the wear of the Ni/Cu multilayer, the high wear resistance can be obtained regardless of the strengths of the multilayers.

Introduction

Multilayered structures whose individual layer thickness is reduced down to nanometer scale have shown excellent mechanical properties including hardness [1], tensile strength [1–3], and fatigue life [4]. It is considered that these enhancements are attributable to high-density parallel interfaces which may behave as barriers against dislocation activities. In addition to these properties, wear resistance is also expected to be improved by surface coating with the metallic multilayers. However, only a few studies have been reported on tribological properties of Ni/Cu multilayers [5, 6].

Evolution of fine-grained microstructure has widely been reported in ductile materials subjected to sliding wear [7–10]. Microstructural aspects of the wear process of the materials were attempted to be understood from observations of worn surface. For the multilayers subjected to sliding wear, both the grain refinement and fragmentation of laminated structure are anticipated. However, the observation of microstructure in the worn multilayer has not been reported as far as we know.

In the present study, sliding wear tests on electrodeposited Ni/Cu multilayers having various layer thicknesses were carried out. Effects of both layer thickness and contacting load on wear resistance were investigated. Microstructures of the worn Ni/Cu multilayers were observed with a scanning ion microscope (SIM) and a transmission electron microscope (TEM). In particular, the authors paid attention to the annihilation of laminated structure to understand the difference between layer thickness dependences of the wear resistance and the Vickers hardness.

T. Hattori (✉)
Material Engineering R&D Department, JTEKT Corporation,
24-1, Kokubuhiganjyo-Cho, Kashiwara, Osaka 582-8588, Japan
e-mail: tomoya_hattori@jtekt.co.jp

T. Hattori · Y. Kaneko · S. Hashimoto
Department of Intelligent Materials Engineering,
Faculty of Engineering, Osaka City University,
Osaka 558-8585, Japan

Experimental procedure

Specimen preparation

A polycrystalline copper of 99.99% purity was used as a substrate, which was annealed at 1,073 K for 2 h in vacuum. After the annealing, the substrate was mechanically and electrolytically polished. A target area for the electrodeposition was limited to an inner site of a circle as indicated in Fig. 1. The other area was insulated with a painting lacquer.

Ni/Cu multilayers and a nickel coating were fabricated by an electrodepositing technique in a single aqueous solution. The solution contained $Ni(H_2NSO_3)_2$, $CuSO_4$ and H_3BO_3. The temperature was kept at 313 K during electrodepositing. Electric current required for the electrodeposition was supplied through a counter electrode of a platinum-plated titanium. The potential of the substrate was controlled to be −30 and −650 mV vs. standard hydrogen electrode (SHE) during the copper and nickel depositions, respectively. Deposition of the Ni/Cu multilayer from the single solution was achieved by the repeatition of alternate potential application at −30 and −650 mV vs. SHE, as shown in Fig. 2. Since the ionization tendency of copper is lower than that of nickel, small amount of copper atoms codeposit during the nickel deposition. In order to minimize the copper codeposition, the concentration of $CuSO_4$ in the solution was set much lower than $Ni(H_2NSO_3)_2$. In this study, ratio of the nickel layer thickness to the copper one was kept to be 1 to 1. Four kinds of the multilayers whose layer thicknesses were $h = 5$, 20, 50, 100 nm were prepared. We also prepared a nickel coating; deposited from the same aqueous solution. The aimed total thicknesses of the multilayers and the nickel coating were set at 5 μm.

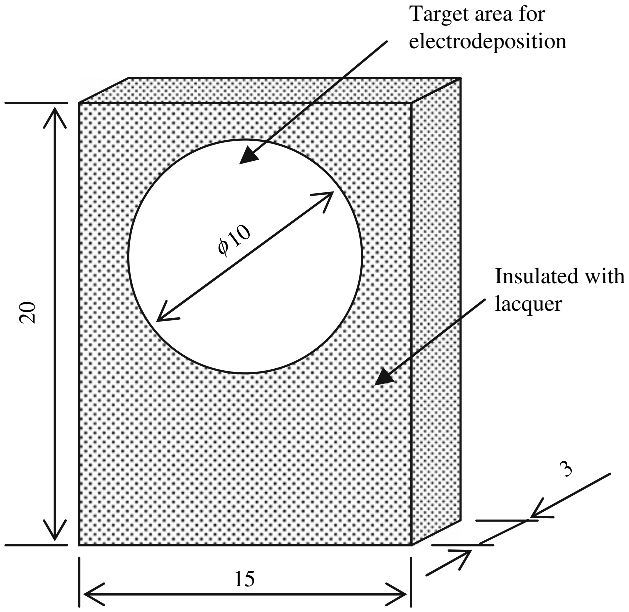

Fig. 1 A schematic illustration of a copper substrate

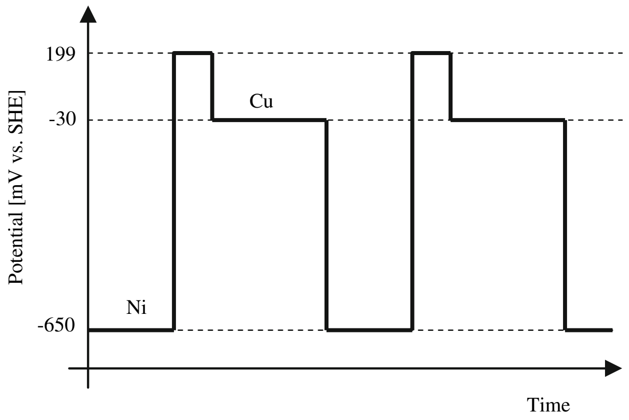

Fig. 2 A potential waveform for the electrodeposition of Ni/Cu multilayer

Wear experiment

Wear experiments were conducted with a ball-on-disk tester in air at room temperature. The specimens which were coated by the multilayers and the nickel were equipped as rotating disks. AISI 52100 steel ball, whose hardness is HRC 62–65 and diameter is 4.8 mm, was used as a counterpart. Before the wear experiments, the specimens were cleaned with ethanol and hexane. The specimen surfaces were lubricated with mineral oil of viscosity grade ISO VG8. A rotating radius was 3 mm and a rotational speed was 50 r.p.m., thus a sliding speed was 15.7 mm/s. The normal loads P were 1 and 5 N. The test duration was 3,600 s, which corresponds to sliding distance $L = 56.5$ m. Ambient temperature during all the tests was kept at the range from 295 to 299 K. After the wear tests, shapes of the wear tracks were measured by a noncontact 3D optical profiler.

Observations of microstructures

In order to investigate the microstructural changes in the multilayers subjected to the sliding wear, the cross section observations of the as-deposited and the worn specimens were carried out. The specimens were cut perpendicular to the sliding direction using a focused ion beam (FIB) system. The cross sections were observed with a scanning ion microscope (SIM) operating in the FIB system and a transmission electron microscope (TEM).

Results and discussion

Fabrication of the Ni/Cu multilayers

Figure 3 shows SIM photographs of the cross sections of the as-deposited Ni/Cu multilayers and the nickel coating. Since intensity of secondary electron yield by gallium ion bombardment is sensitive to atomic number Z of a target material [11], we can distinguish the nickel layer from the copper layer in the SIM photograph. Bright images in the SIM photographs correspond to the copper layer. The individual layers were visible at least in the layer thicknesses of 50 and 100 nm. At the multilayers of 5 nm and 20 nm layer thickness, however, an identification of individual layer was difficult because the SIM resolution is insufficient. In our previous TEM observation [1], the stack of Ni and Cu layers was recognized even in the multilayer having 5 nm layer thickness. Hence, the present multilayers with $h = 5$ nm and 20 nm should have the layered structures. It is noted that the 5 nm multilayer had a polycrystal-like structure unlike the other multilayers. The total thickness measured from the SIM observations are listed in Table 1. The total thicknesses were deviated from 5 μm which was the desired thickness at the electrodeposition. Since the growth rate of an electrodeposit depends on an orientation of grains of the copper substrate, the total thickness varied even in the same specimen. This grain orientation dependence would be one reason for the observed deviations from 5 μm total thickness.

Wear properties

Cross sectional profiles of wear tracks are shown in Fig. 4. Grooves induced by sliding wear can be recognized in all the specimens tested. All the grooves of the multilayers were shallower than that of the nickel coating for both $P = 1$ N and 5 N conditions. Figure 5 shows the schematics of a FIB machining area for SIM observation below a wear track. Wear tracks were cut perpendicular to sliding direction at the center of the wear tracks. Figures 6 and 7 show the SIM images at the center of cross sections of the wear tracks at the test conditions of $P = 1$ N and 5 N,

Table 1 Total film thicknesses before and after the wear tests

Test conditions	Specimens	Before wear test, t_A (μm)	After wear test, t_B (μm)	Wear depth, Δt (μm)
$P = 1$ N	$h = 5$ nm	4.2 ± 0.43	4.0 ± 0.08	0.2
	$h = 20$ nm	4.7 ± 0.45	4.5 ± 0.21	0.2
	$h = 50$ nm	4.0 ± 0.34	4.2 ± 0.54	−0.2
	$h = 100$ nm	4.7 ± 0.54	4.2 ± 0.28	0.5
	Ni coating	5.7 ± 0.38	4.4 ± 0.36	1.3
$P = 5$ N	$h = 5$ nm	5.0 ± 0.70	4.8 ± 0.30	0.2
	$h = 20$ nm	5.3 ± 0.30	4.8 ± 0.15	0.5
	$h = 50$ nm	4.0 ± 0.22	3.7 ± 0.67	0.3
	$h = 100$ nm	3.9 ± 0.57	2.8 ± 1.05	1.1
	Ni coating	5.0 ± 0.47	0	5.0

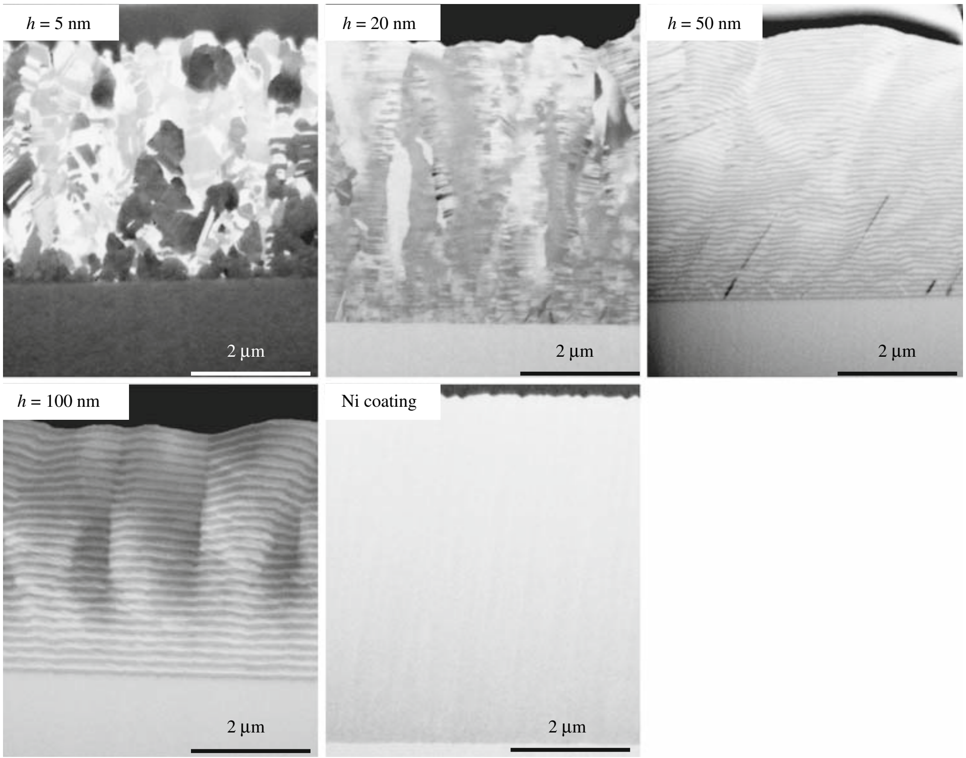

Fig. 3 SIM photographs of cross sections of the as-deposited Ni/Cu multilayers and the as-deposited Ni coating

Fig. 4 Cross sectional profiles of wear tracks of (**a**) $P = 1$ N and (**b**) $P = 5$ N

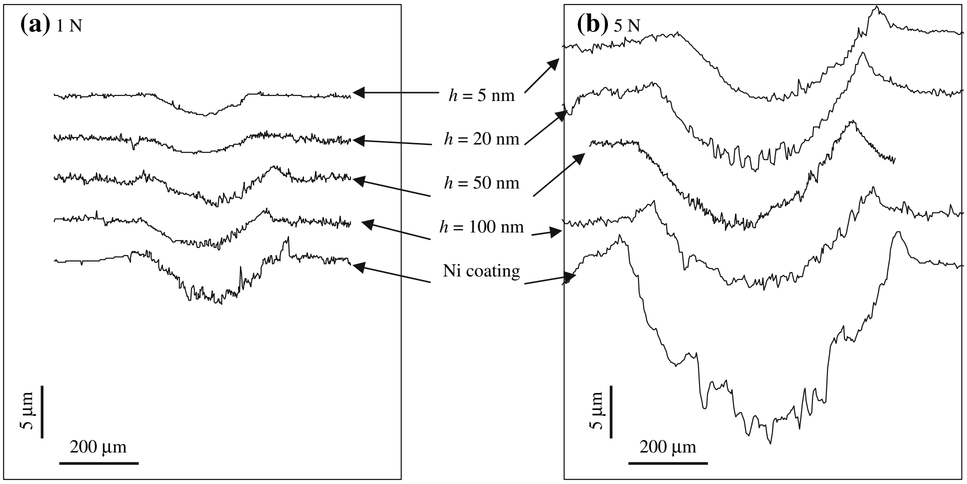

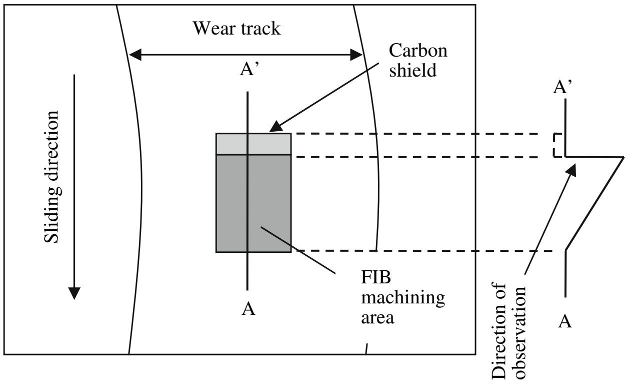

Fig. 5 Schematic illustration of FIB machining area for observation below a wear track. Wear tracks were cut perpendicular to sliding direction at the center of the wear tracks

respectively. In order to determine the wear resistance of the surface coatings, the residual layer thicknesses were measured. Table 1 shows the wear depth at the center of the wear tracks. Since the multilayer films remained after the wear tests, the surface grooves at the wear tracks (Fig. 4) were caused mostly by the deformation of the copper substrates. The wear depths of all the multilayers were smaller than that of the nickel coating at both the loading conditions. It should be noted that the nickel coating was entirely removed at $P = 5$ N, although the multilayer structures still remained. It was found that the wear depths in the multilayers were less than one-fifth of that of a conventional nickel coating at $P = 5$ N. These results prove that the wear resistances of the multilayers are superior to that of the nickel coating. The wear resistance of the multilayer was almost independent of the component layer thickness, except the multilayer of $h = 100$ nm whose resistance was lower than those of the others.

In our previous Vickers hardness tests on the Ni/Cu multilayers [1], the hardness decreased rapidly with decreasing layer thickness when the layer thickness was less than 10 nm. The hardness at $h = 5$ nm was certainly lower than those of $h = 10$ nm and 100 nm. The softening observed at $h = 5$ nm is not clearly understood. One of the possible explanations is the annihilation of misfit dislocation networks—which offer resistance to interface cutting by dislocation—at the short layer thickness [12]. In spite of the low Vickers hardness, the wear resistance of the multilayer of $h = 5$ nm was comparable to the other multilayers. The layer thickness dependence of the wear resistance was different from that of the Vickers hardness.

Subsurface microstructure below the wear tracks

SIM observations below the wear tracks revealed that a lot of equiaxed grains—which have been observed in wear experiments on ductile materials [8, 9]—were generated in the multilayers and the nickel coatings as shown in Figs. 6 and 7. The grain formations in the multilayer was limited near the worn surface, as clearly seen in $h = 100$ nm (Fig. 6), while the nickel coating contained the grains throughout thickness. These grains should be produced by severe plastic deformation due to the sliding wear. Thicknesses of the grained area are summarized in Table 2. The grained area in the multilayer tended to broaden as the layer thickness increased. It is likely that the wear resistance presented in Table 1 increased with decreasing thickness of the grained area. The difference thicknesses of the grained area thickness is partially understood from the layer thickness dependence of strength in the Ni/Cu multilayer, at which the hardness increased with decreasing layer thickness at the layer thickness $h > 10$ nm [1]. A lot of parallel Ni/Cu interfaces in the multilayers would act as barriers against the dislocation movements [13], which are necessary for the formation of the grains. However, the thin

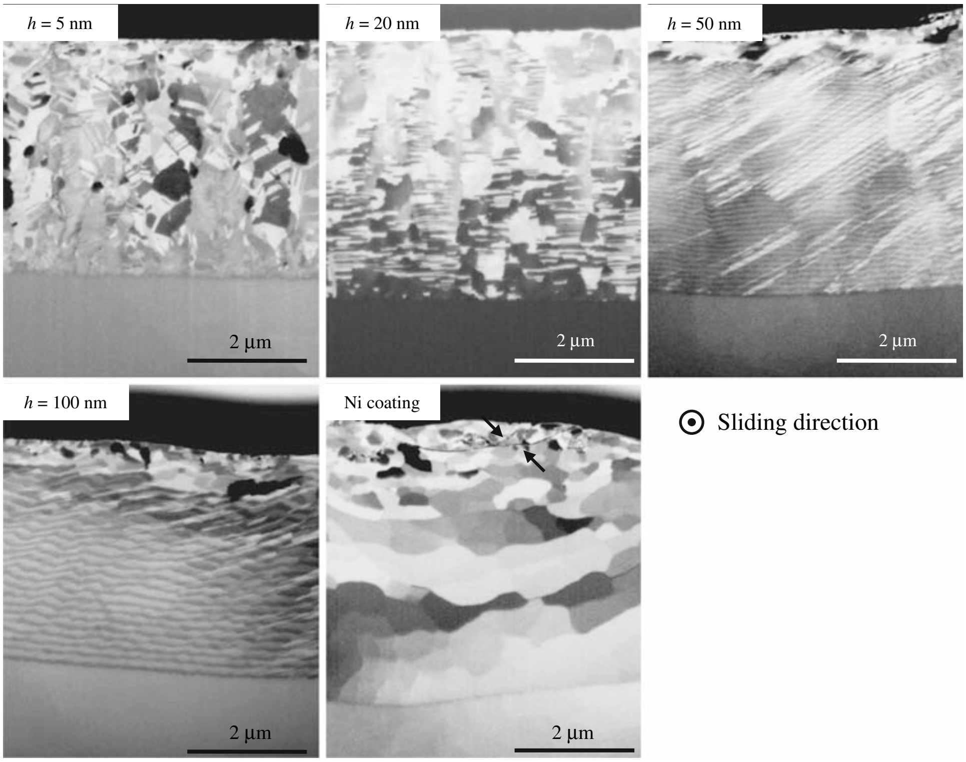

Fig. 6 SIM photographs showing cross sections below the wear track of the Ni/Cu multilayers and the nickel coating, where the wear tests were conducted at $P = 1$ N. Arrows indicate cracks. Sliding directions are perpendicular to the cross sections for all the photographs

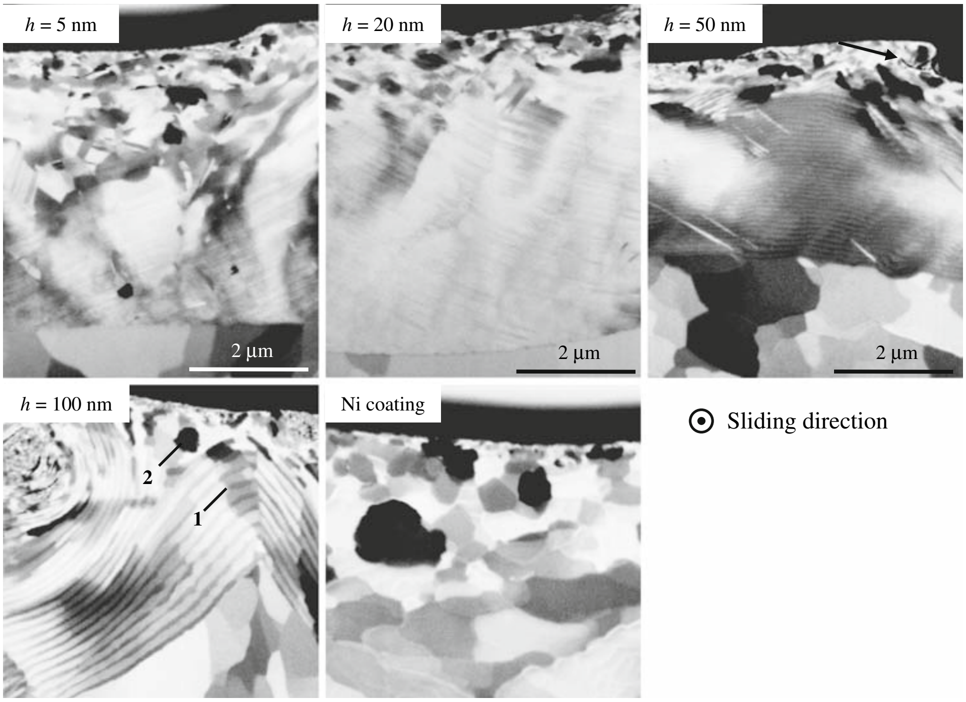

Fig. 7 SIM photographs showing cross sections below the wear track of the Ni/Cu multilayers and the nickel coating, where the wear tests were conducted at $P = 5$ N. An arrow indicates a crack. Sliding directions are perpendicular to the cross sections for all the photographs. Grain 1 in the 100 nm multilayer had a laminated structure and the misorientation from the surrounding multilayer was small. On the other hand, no laminated structure is visible in Grain 2 of the 100 nm multilayer. The photograph of the "Ni coating" actually shows the copper substrate because the nickel coating was removed by the wear test

grained area at $h = 5$ nm is inconsistent with the low Vickers hardness [1].

The grains formed during the wear process can be classified into two types as indicated in Fig. 7. One has the laminated structure inside the grain (Grain 1 in Fig. 7). Misorientation from the surrounding grains seems small, because the difference in brightness intensity was little. The grains of this kind should be generated as a result of dislocation cell formation induced by plastic deformation. In the grains of the other type, there is no appreciable laminated structure. The brightness of the grain without the laminated structure (Grain 2 in Fig. 7) differed considerably from neighboring grains, thus the grain should have a large misorientation.

Table 2 Thickness of grained area formed by sliding wear

Specimens	Thickness of grained area in the films (μm)	
	$P = 1$ N	$P = 5$ N
$h = 5$ nm	<0.1	0.6
$h = 20$ nm	<0.1	1.1
$h = 50$ nm	1.0	1.6
$h = 100$ nm	1.4	2.7
Ni coating	4.4	No nickel coating remained

Several cracks were observed at the worn surface of the nickel and the multilayer as indicated in Figs. 6 and 7 by arrows, respectively. Although the 100 nm multilayer deformed significantly at $P = 5$ N, no cracks were found in the laminated structure region where the fine grains were absent. The crack formations were detected only at the areas which contained the fine grains. Accordingly, it seems likely that the surface cracks were grown only in the fine-grained areas in both the Ni/Cu multilayers and the nickel coating. The cracked areas would be peeled during the wear process. Hence, the wear resistance can be inversely proportional to the thickness of the grained area where the cracks can be formed. This is consistent with the relationship between the wear depth (Table 1) and the grained area thickness (Table 2).

Figure 8 shows bright field TEM images of the $h = 100$ nm multilayer worn at $P = 5$ N. The cross sections both near the copper substrate and near the worn surface were observed. In the TEM photograph of the neighborhood of the substrate, the laminated structure still remained, as well as the SIM observation. From an electron diffraction pattern obtained near the substrate, the Ni/Cu multilayer had a textured structure. On the other hand, the laminated structure was annihilated near the worn surface; the Ni/Cu multilayer may became a Ni–Cu alloy due to the sliding wear process. Instead of the laminated structure, formations of the equiaxed grains are recognized. Since the electron diffraction pattern indicates that the equiaxed grains had no preferential orientations, the equiaxed grains must be have large misorientations from the neighboring grains.

It had been proposed that dynamic recrystallization can occur at surface layer which is subjected to wear process [7, 14]. The formation of the present equiaxed grains without the laminated structure can also be understood from the dynamic recrystallization occurring in the following manner. If the Ni/Cu multilayer is subjected to severe plastic deformation induced by the sliding wear, the laminated structure would be annihilated owing to a process like a mechanical alloying. During the sliding wear, high-density lattice defects and frictional heat near contacting surface will be generated at the same time. Since promoted by both the high-density defects and the increase in temperature, the dynamic recrystallization can occur after the annihilation period of the laminated structure. The large misorientations between the equiaxed grains are also consistent with the recrystallization.

Figure 9 shows sizes of the generated grains in $h = 50$ nm and 100 nm multilayers and the nickel coating, plotted against the distance from the worn surface. In all the specimens observed, small grains were generated near the worn surface. The 100 nm multilayer tested at 5 N exhibited a distribution clearly different from the other multilayers. This is because the entire multilayer was bent significantly as seen in Fig. 7. Hence, several large grains which were originally located at deeper areas appeared near the surface, and the grains generated near surface moved to the deeper areas. We paid attention to the grain sizes in the 50 nm and 100 nm multilayers tested at the same contact load ($P = 1$ N). Many large grains were detected in the 100 nm multilayer, in comparison with the 50 nm multilayer. If the grain refinement is achieved by the dislocation cell formation induced by plastic deformation, the observed large grain size at the 100 nm multilayer is inconsistent with the fact that the hardness of the 100 nm

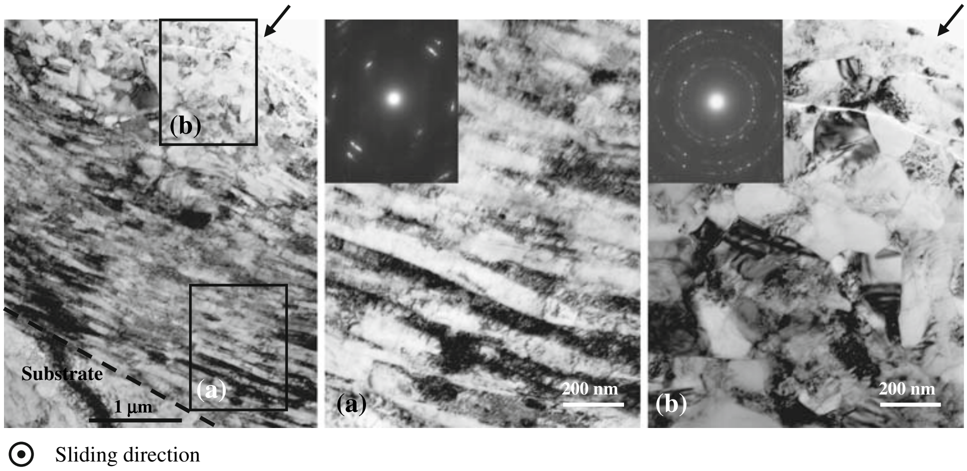

Fig. 8 Bright field TEM images of a cross section below the wear track of the $h = 100$ nm multilayer tested at $P = 5$ N. Sliding directions are perpendicular to the cross sections for all the photographs. The cross section (**a**) near the copper substrate and (**b**) near the worn surface was observed. An arrow indicates the worn surface

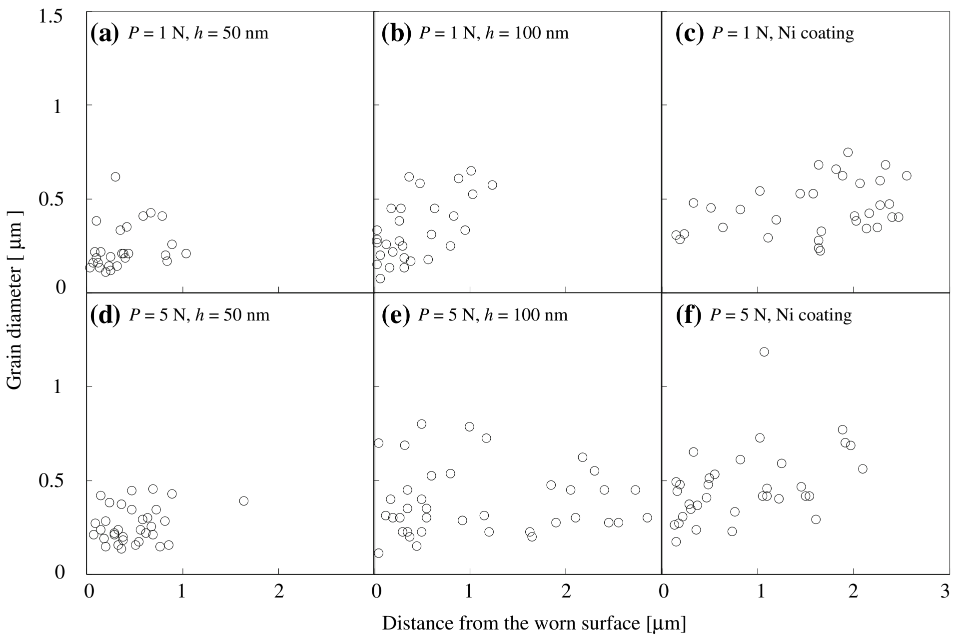

Fig. 9 Diameters of the grains which were generated by the sliding wear experiments

multilayer was lower than that of 50 nm. The brightness intensities of the large grains in the 100 nm multilayer mostly differed from those of the neighboring grains, although there was no significant difference between the brightness intensities of the grains in the 50 nm multilayer, as shown in the Fig. 6. These results mean that the 100 nm multilayer may contain many recrystallized grains, with compared to the 50 nm multilayer. Hence, the large grains measured in the 100 nm multilayer can be interpreted by the dynamic recrystallization, because the plastic deformation leading to the dynamic recrystallization should be more severe in the 100 nm multilayer than in the 50 nm multilayer having the high strength.

The microstructure of the worn Ni/Cu multilayer was characterized by the annihilation of the laminated structure as seen in the TEM observation. The fine grains with large misorientation angle and subsequent surface cracking presumably occurred after the annihilation of the laminated structure: the annihilation period of the laminated structure would precede the surface removal period. A wear process of the usual single-phase material does not require this annihilation period. Assuming that the wear of the Ni/Cu multilayer must involve the annihilation period of the laminated structure, one can understand the high wear resistance of the 5 nm multilayer at which the Vickers hardness was low.

Conclusions

Sliding wear tests were conducted on the Ni/Cu multilayers having the component layer thickness *h* ranging from 5 nm to 100 nm, which were fabricated by the elecrodeposition technique. From the investigation on the wear resistance and the microstructures of the Ni/Cu multilayers, following conclusions are obtained.

(1) The cross section profiles and the reduction in film thickness were measured after the sliding wear tests. It was found that the wear depth in the multilayers was less than one-fifth of that of a conventional nickel coating at $P = 5$ N. The wear resistance of the multilayer was almost independent of the component layer thickness, except the multilayer of $h = 100$ nm whose resistance was lower than those of the others.

(2) The grains were generated locally near the worn surface in the multilayers and the nickel coating. The surface cracks were grown in such grained areas. The multilayer where the grained area was large showed a low wear resistance.

(3) In the SIM observations, the grains formed by the sliding wear could be classified into two types. One had no laminated structure inside the grain. In the other grain type, the laminated structure still remained and the misorientation from the surrounding matrix was small. From the electron diffraction pattern in the TEM observation, the equiaxed grains without the laminated structure existing near worn surface had large misorientations from neighboring grains. It is conceivable that the equiaxed grains without the laminated structure were formed due to dynamic recrystallization occurring after the laminated structure was annihilated by severe deformation.

(4) The wear process of the Ni/Cu multilayer was characterized by the annihilation of the laminated

structure. Assuming that the annihilation period is required for the wear of the Ni/Cu multilayer, the high wear resistance can be understood even for the multilayer having a low strength.

Acknowledgement This work was financially supported by the MEXT Grants-In-Aid for Scientific Research (#16760573).

References

1. Kaneko Y, Mizuta Y, Nishijima Y, Hashimoto S (2005) J Mater Sci 40:3231
2. Menezes S, Anderson DP (1990) J Electrochem Soc 137:440
3. Tench DM, White JT (1991) J Electrochem Soc 138:3757
4. Ebrahimi F, Liscano AJ (2001) Mater Trans 42:120
5. Ruff AW, Myshkin NK (1989) ASME J Tribol 111:156
6. Ruff AW, Lashmore DS (1991) Wear 151:245
7. Dautzenberg JH (1980) Wear 60:401
8. Heilmann P, Clark WAT, Rigney DA (1983) Acta Metall 31:1293
9. Ohno Y, Kaneko Y, Hashimoto S (2006) Mater Sci Forum 503–504:727
10. Prasad SV, Michael JR, Christenson TR (2003) Scripta Mater 48:255
11. Ohya K, Ishitani T (2003) Nucl Instr Mech In Phys Res B 202:305
12. Misra A, Verdier M, Lu YC, Kung H, Mitchell TE, Nastasi M, Embury JD (1998) Scripta Mater 39:555
13. Kaneko Y, Hirota S, Hashimoto S (2007) Key Eng Mater 353–358:1086
14. Hughes DA, Dawson DB, Korellis JS, Weingarten LI (1994) J Mater Eng Perfom 3:459